Study Of The Phytoplankton Plume Dynamics Off The Crozet Islands (Southern Ocean): A Geochemical-Physical Coupled Approach

Virginie Sanial, Pieter van Beek, B. Lansard, Francesco d'Ovidio, Élodie Kestenare, M. Souhaut, Meng Zhou, Stéphane Blain

AGU PUBLICATIONS

JGR

Journal of Geophysical Research: Oceans

RESEARCH ARTICLE

10.1002/2013JC009305

Key Points:
- Study of the natural iron fertilization in the Southern Ocean
- Combined geochemical-physical approach to investigate the exchange rates of waters

Correspondence to:
V. Sanial,
virginie.sanial@legos.obs-mip.fr

Citation:
Sanial, V., P. Beek, B. Lansard, F. d'Ovidio, E. Kestenare, M. Souhaut, M. Zhou, and S. Blain (2014), Study of the phytoplankton plume dynamics off the Crozet Islands (Southern Ocean): A geochemical-physical coupled approach, *J. Geophys. Res. Oceans*, *119*, 2227–2237, doi:10.1002/2013JC009305.

Received 26 JULY 2013
Accepted 21 MAR 2014
Accepted article online 25 MAR 2014
Published online 10 APR 2014

Study of the phytoplankton plume dynamics off the Crozet Islands (Southern Ocean): A geochemical-physical coupled approach

Virginie Sanial[1], Pieter van Beek[1], Bruno Lansard[2], Francesco d'Ovidio[3], Elodie Kestenare[1], Marc Souhaut[1], Meng Zhou[4], and Stéphane Blain[5]

[1]Laboratoire d'Etudes en Géophysique et Océanographie Spatiales (CNRS-CNES-IRD-UPS), Observatoire Midi Pyrénées, Toulouse, France, [2]Laboratoire des Sciences du Climat et de l'Environnement (IPSL-CEA-CNRS-UVSQ), Gif-sur-Yvette, France, [3]LOCEAN-IPSL, Laboratoire d'Océanographie et du Climat (CNRS-IRD-UPMC-MNHN), Paris Cedex, France, [4]Department of Environment Earth and Ocean Sciences, University of Massachusetts Boston, Boston, Massachusetts, USA, [5]Laboratoire d'Océanographie Microbienne (CNRS-UPMC), Observatoire de Banyuls-sur-Mer, Banyuls s/mer, France

Abstract The Crozet Archipelago, in the Indian sector of the Southern Ocean, constitutes one of the few physical barriers to the Antarctic Circumpolar Current. Interaction of the currents with the sediments deposited on the margins of these islands contributes to the supply of chemical elements—including iron and other micro-nutrients—to offshore high-nutrient, low-chlorophyll (HNLC) waters. This natural fertilization sustains a phytoplankton bloom that was studied in the framework of the KEOPS-2 project. In this work, we investigated the time scales of the surface water transport between the Crozet Island shelves and the offshore waters, a transport that contributes iron to the phytoplankton bloom. We report shelf-water contact ages determined using geochemical tracers (radium isotopes) and physical data based on in situ drifter data and outputs of a model based on altimetric Lagrangian surface currents. The apparent ages of surface waters determined using the three independent methods are in relatively good agreement with each other. Our results provide constraints on the time scales of the transport between the shelf and offshore waters near the Crozet Islands and highlight the key role played by horizontal transport in natural iron fertilization and in defining the extension of the chlorophyll plume in this HNLC region of the Southern Ocean.

1. Introduction

The Southern Ocean is known as the largest high-nutrient, low-chlorophyll (HNLC) region of the global ocean. While nutrient concentrations (nitrate, phosphate, and silicic acid) are high, the phytoplankton development is paradoxically low in these areas. Light-limitation [*Mitchell et al*., 1991], grazing-control [*Frost*, 1991; *Banse*, 1996], and iron-limitation [*Martin et al*., 1990; *de Baar et al*., 1995] have been proposed as hypotheses to explain this pattern. Even if each factor plays a significant role [*Boyd*, 2002], artificial iron fertilization experiments confirmed that the low iron concentration of the Southern Ocean waters limits the phytoplankton growth [see e.g., *Coale et al*., 1996; *Boyd et al*., 2000]. Areas with relatively high chlorophyll concentrations can however be found in this HNLC ocean and are located in the vicinity of subantarctic islands [*Blain et al*., 2001; *Lucas et al*., 2007; *Seeyave et al*., 2007]. Phytoplankton blooms thus take place off the Crozet Islands [*Pollard et al*., 2002], off the Kerguelen Islands [*Blain et al*., 2001] and off the South Georgia [*Korb and Whitehouse*, 2004; *Korb et al*., 2004]. These phytoplankton blooms were investigated during the CROZEX project (CROZet natural iron bloom and EXport experiment) [*Pollard et al*., 2007a], the KEOPS project (KErguelen Ocean comPared Study) [*Blain et al*., 2007], and the U.S. AMLR Program (Antarctic Marine Living Resources) [*Dulaiova et al*., 2009], respectively. These latter studies concluded that the phytoplankton development was promoted by the input of iron released by sediments deposited on the margins. Such phytoplankton blooms constitute a sink for atmospheric carbon dioxide and, therefore, play an important role in the carbon cycle and in the regulation of the climate system [*Blain et al*., 2007; *Pollard et al*., 2007a].

Previous studies of natural iron fertilization have relied on the use of geochemical tracers such as radium isotopes (^{224}Ra, $T_{1/2}$ = 3.66 days; ^{223}Ra, $T_{1/2}$ = 11.4 days; ^{228}Ra, $T_{1/2}$ = 5.75 years; ^{226}Ra, $T_{1/2}$ = 1600 years) to trace and quantify the input of iron delivered to open-ocean waters [*Charette et al*., 2007; *van Beek et al*., 2008; *Dulaiova et al*., 2009]. The four radium isotopes are produced in the sediments by the decay of particle-

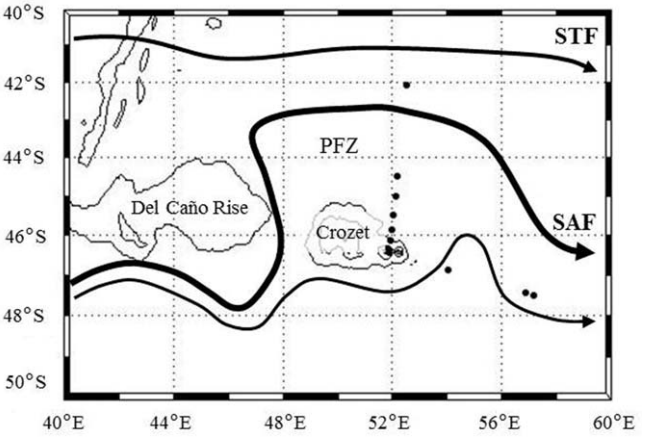

Figure 1. Schematic of the circulation around the Crozet Islands, slightly modified from *Pollard et al.* [2007b]. SAF, SubAntarctic Front; STF, SubTropical Front; and PFZ, Polar Frontal Zone. Stations investigated during the cruise are reported on the map.

bound thorium isotopes and diffuse out of the sediments. Therefore, waters lying above the sediments are enriched in radium as well as in iron and in other micronutrients that are also released from the sediments. These elements may then be transported by diffusion and advection toward offshore waters. While iron may be removed from the water column by biotic or abiotic processes, radium behaves as a conservative tracer. Very few studies, however, reported activities of ^{224}Ra and/or ^{223}Ra in the Southern Ocean, although these isotopes are powerful tools to investigate time scales in the order of several days to 2–3 months [*Charette et al.*, 2007; *Dulaiova et al.*, 2009; *Annett et al.*, 2013]. The half-life of these isotopes is short (3.66 and 11.4 days, respectively) and their analysis in open-ocean waters is thus challenging. Despite a longer half-life (5.75 years), ^{228}Ra activities are also particularly low ($<$0.1 dpm/100 L) in the Southern Ocean [*Kaufman et al.*, 1973].

The development of the phytoplankton bloom that takes place annually off the Crozet Islands is a good case study for investigating the impact of the natural iron fertilization associated with islands located in HNLC waters. Phytoplankton blooms develop north of the Crozet Plateau between early and mid-September, peaking in late October, and declining throughout November [*Venables et al.*, 2007]. The Crozet Islands are identified as the major source of the iron that sustains the phytoplankton bloom [*Planquette et al.*, 2007]. The flux of dissolved iron transported to the bloom area by advection, vertical mixing, and atmospheric deposition was estimated during the CROZEX project at 551 nmol Fe m^{-2} d^{-1} when normalized to a bloom area of 90,000 km^2 [*Charette et al.*, 2007; *Planquette et al.*, 2007]. This iron input, combined with the existence of a zone of weak circulation over the Crozet Plateau, allows the phytoplankton bloom to develop during austral spring by tapping into the iron supply formed during the winter season [*Pollard et al.*, 2002].

The large-scale horizontal circulation patterns in the region of the Crozet Islands were described during the CROZEX project [*Pollard et al.*, 2007b]. Horizontal advection was shown to play a significant role in the redistribution of iron-enriched waters in the Crozet Islands region [*Charette et al.*, 2007; *Pollard et al.*, 2007b]. For this reason, we propose to use three independent methods to estimate the transport of chemical elements toward offshore waters. In this work, the four radium isotopes were analyzed in surface seawater samples collected off the Crozet Islands in order (i) to track the geochemical signature of surface waters, using radium isotopes as a proxy for sediment-derived iron inputs and (ii) to determine the apparent ages for the offshore waters which in turn give us information on the time scales of the transport between the shelf waters and the open ocean. Apparent ages, determined using radium isotopes, were then compared to in situ data derived from a drifter released off the Crozet Island and to outputs of a Lagrangian model based on altimetric surface current data.

2. Materials and Methods

2.1. The KEOPS-2 Project

The KEOPS-2 project took place during austral spring 2011 (between 14 October and 23 November) on board of the R/V Marion Dufresne (IPEV: Institut Polaire Français—Paul Emile Victor and TAAF: Terres Australes et Antarctiques Françaises). The KEOPS-2 project was a GEOTRACES process study designed to study the mechanisms of natural iron fertilization off Kerguelen Islands and its impact on ecosystems and biogeochemical cycles. A short visit to the Crozet Islands during that cruise (14–16 October 2011) provided the

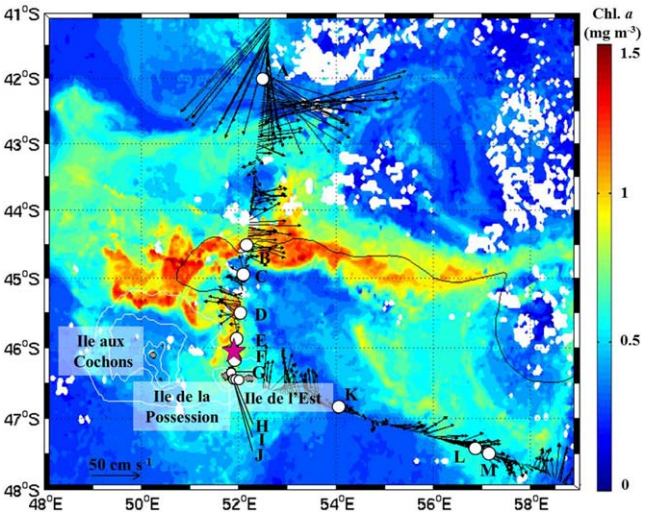

Figure 2. Satellite composite image of sea surface chlorophyll *a* (mg m^{-3}) around the Crozet Islands on 14 October 2011. Solid white lines mark the 200, 500, and 2000 m bathymetric contours. White dots represent the stations where seawater samples were collected for radium analysis. The arrows show the currents derived from S-ADCP vectors. The drifter trajectory is highlighted by the black line and its deployment location is shown with the magenta star.

opportunity to study the phytoplankton plume in that area. The KEOPS-2 project followed up the first KEOPS project, which was conducted in 2005 [*Blain et al*., 2007].

2.2. Study Area

The Crozet Plateau is located in the Indian sector of the Southern Ocean and is one of the few physical barriers for the eastward-flowing Antarctic Circumpolar Current (ACC). The Crozet Plateau (150 km wide) is shallower than 500 m depth [*Pollard et al*., 2007a] and is divided into two plateaus (eastern and western plateaus). Two volcanic islands are located on the eastern plateau: Ile de la Possession (46°24′S; 51°46′E) and Ile de l'Est (46°25′S; 52°12′E). The main island of the western plateau is Ile aux Cochons (46°06′S; 50°14′E). Here the term "Crozet Islands" is used to refer to all the islands located on the Crozet Plateau. When the ACC reaches the Crozet Plateau, it is separated into two subcurrents: the major branch is associated with the SubAntarctic Front (SAF) and the other branch flows south of the Crozet Plateau along 47°S [*Pollard et al*., 2007a] (Figure 1). The SAF heads to the north between the Del Caño Rise and the Crozet Plateau toward 43°S, and then propagates eastward. The southern SubTropical Front (STF) and the Polar Front (PF) flow at 41°S and 50°S, respectively [*Pollard and Read*, 2001]. SubAntarctic Surface Water (SASW) covers the investigated area between the STF and the PF [*Emery and Meincke*, 1986; *Castrillejo et al*., 2013]. Two transects were made north and south-east of the eastern Crozet Plateau (Figure 1). The physical observations described below as well as the collection of seawater samples were performed along these two transects.

2.3. Radium Activities

2.3.1. Sample Collection

We collected water samples inside and outside the chlorophyll plume according to real-time chlorophyll satellite images (Figure 2). Surface seawater samples (250–500 L) were collected at 7 m depth using a clean pump designed by IPEV (Institut Paul Emile Victor), and were placed in large plastic tanks. Two samples (45.2 and 22.7 L) were also collected directly on the beach of the Baie du Marin, on Ile de la Possession (Table 1). These seawater samples were then passed by gravity through cartridges filled with MnO_2-impregnated acrylic fibers ("Mn-fibers") following *Moore* [2008]. The flow rate was fixed at $\leq$0.5 L min^{-1} to provide 100% extraction efficiency [*Moore*, 2008; *van Beek et al*., 2010]. The Mn-fibers were then rinsed with MilliQ water and dried partially before analysis.

2.3.2. Sample Analysis

The Mn-fibers were analyzed using a Radium Delayed Coincidence Counter system (RaDeCC) [*Moore and Arnold*, 1996]. The first counting was performed on board the ship immediately after sampling to quantify both ^{223}Ra and ^{224}Ra activities and a second counting was done 3 weeks after sampling to quantify the ^{224}Ra supported by ^{228}Th [*Moore*, 2000a]. A third counting of the samples was performed in the laboratory at Toulouse, 3 months after the initial sample collection, to estimate the ^{223}Ra supported by ^{227}Ac. ^{224}Ra and ^{223}Ra activities were corrected for the ^{224}Ra supported by ^{228}Th and the ^{223}Ra supported by ^{227}Ac, respectively. Excess ^{224}Ra and ^{223}Ra activities are reported in Table 1 (denoted $^{224}Ra_{ex}$ and $^{223}Ra_{ex}$, respectively). The ^{224}Ra and ^{223}Ra activities described in section 3 refer to these "excess radium activities." Uncertainties for both isotopes were calculated following *Garcia-Solsona et al*. [2008] and were reported with a one-sigma confidence interval.

Table 1. Radium Activities and Apparent Ages Determined in Surface Seawater Samples Collected off the Crozet Islands[a]

Station	Latitude	Longitude	Distance from Crozet (km)	Volume (L)	Station Depth (m)	SSS	SST (°C)	$^{223}Ra_{ex}$ (dpm/100 L)	$^{224}Ra_{ex}$ (dpm/100 L)	^{228}Ra (dpm/100 L)	^{226}Ra (dpm/100 L)	$^{224}Ra_{ex}/^{228}Ra$	$^{224}Ra_{ex}/^{223}Ra_{ex}$	Apparent Ages $^{224}Ra_{ex}/^{228}Ra$ (Days)	Apparent Ages $^{224}Ra_{ex}/^{223}Ra_{ex}$ (Days)	Apparent Ages Model (Days)	Apparent Ages Drifter (Days)
A	−42.0620	52.5280	488	450	3986	35.300	13.27	<DL	<DL	0.736 ± 0.04	6.3 ± 0.05			>30	>30	>120	
B	−44.5100	52.1717	214	450	3418	33.864	4.07	0.043 ± 0.010	0.039 ± 0.060	0.090 ± 0.01	13.1 ± 0.05	0.43 ± 0.67	0.91 ± 1.41	8 ± 8	21 ± 12	21 ± 2	27
C	−44.9997	52.1007	160	450	3262	33.833	3.77	<DL	<DL	0.149 ± 0.02	12.2 ± 0.05			>30	>30	>120	
D	−45.4967	52.0295	105	450	2962	33.870	3.93	<DL	<DL	0.169 ± 0.02	13.1 ± 0.06			>30	>30	27 ± 15	7
E	−45.8812	51.9745	62	450	3012	33.881	4.11	<DL	0.034 ± 0.029	0.052 ± 0.01	13.1 ± 0.06	0.66 ± 0.59		6 ± 5	>30	9 ± 11	3
F	−46.1393	51.9370	34	450	2027	33.888	4.11	0.022 ± 0.007	0.051 ± 0.035	0.134 ± 0.02	14.1 ± 0.05	0.38 ± 0.27	2.32 ± 1.75	9 ± 4	14 ± 6	2 ± 1	0
G	−46.3310	51.8433	12	450	168	33.888	4.21	<DL	0.044 ± 0.035	0.207 ± 0.03	14.5 ± 0.06	0.21 ± 0.17		12 ± 4	>30	0	
H	−46.4258	51.8730	1	450	150	33.901	4.11	0.029 ± 0.01	0.428 ± 0.03	0.175 ± 0.02	7.1[b] ± 0.05	2.45 ± 0.34	14.76 ± 4.18	0	0	0	
I	−42.4258	51.8612	0	45.2	Beach	31.552	ND	0.145 ± 0.05	2.117 ± 0.18	1.106 ± 0.02	13.5 ± 0.20	1.91 ± 0.29	14.60 ± 4.90	0	0	0	
J	−46.4263	51.8614	0	22.7	Beach	30.560	ND	0.185 ± 0.09	2.421 ± 0.25	1.456 ± 0.14	14.2 ± 0.29	1.66 ± 0.31	13.09 ± 6.44	0	0	0	
K	−46.8790	54.0400	173	500	3738	33.833	3.50	<DL	<DL	0.233 ± 0.22	10.0 ± 0.06			>30	>30	>120	
L	−47.4000	56.8530	394	450	4386	33.809	4.72	<DL	<DL	0.084 ± 0.03	12.1 ± 0.06			>30	>30	72 ± 8	
M	−47.5000	57.1580	418	450	4350	33.804	4.82	<DL	0.019 ± 0.018	0.103 ± 0.02	8.5[b] ± 0.05	0.18 ± 0.18		>30	>30	>120	

[a] <DL, below the detection limit; ND, not determined; SST, sea surface temperature; SSS, sea surface salinity. We reported ">30 days" for samples that did not contain any remaining ^{224}Ra suggesting waters older than 30 days. Apparent ages derived from the model were averaged on a 0.1° latitude × 0.1° longitude window. The errors associated with these ages are the standard deviation of the mean calculated in that window.

[b] We cannot exclude a low extraction efficiency for these samples.

Following the analysis of ^{223}Ra and ^{224}Ra using RaDeCC, ^{226}Ra and ^{228}Ra activities were determined using low-background gamma detectors placed at the LAFARA underground laboratory in the French Pyrénées [*van Beek et al.*, 2010, 2013]. The Mn-fibers were either (i) ashed at 820°C for 16 h [*Charette et al.*, 2001] and analyzed using a well-type germanium detector or (ii) compressed and analyzed using a semiplanar detector [*van Beek et al.*, 2013]. ^{226}Ra activities were determined using the ^{214}Pb (295 and 352 keV) and the ^{214}Bi (609 keV) peaks. ^{228}Ra activities were determined using ^{228}Ac peaks (338, 911, and 969 keV). The counting interval for each sample was ca. 120 h to allow the quantification of the low ^{228}Ra activities. The uncertainties reported for gamma counting consist of the error associated with counting statistics (one sigma). The radium activities reported here are expressed in disintegration per minute and per 100 L of seawater (dpm/100 L).

2.4. Physical Data

2.4.1. S-ADCP Data

The major zonal and meridional current velocity profiles along the transects conducted off Ile de la Possession were identified using the 75 kHz narrow band model from the "Ocean Surveyor" Shipboard Acoustic Doppler Current Profiler (S-ADCP) of the R/V Marion Dufresne. The data treatment was done using a CODAS-3 code (Common Oceanographic Data Access System, version 3) developed at the University of Hawaii. The procedure and software of the processing are freely available at http://currents.soest.hawaii.edu/. S-ADCP data were corrected from tide effects using a barotropic, time-stepping, and nonlinear regional tidal model [*Maraldi et al.*, 2007].

2.4.2. Thermosalinograph Data

Underway thermosalinograph (TSG) provided sea surface temperature (SST) and sea surface salinity (SSS) measurements. The instrument was mounted on the ship hull at 7 m depth. Data were averaged every 5 min. The calibration of these data was performed before and after the cruise using the temperature and salinity data obtained with a CTD probe attached on the rosette and placed at 7 m depth.

2.4.3. Surface Drifter

A drifter (World Ocean Circulation Experiment, WOCE, Surface Velocity Program, SVP) was released north of Ile de la Possession at 51°56.82′E and 46°04.19′S on 15 October 2011. This drifter was provided by the US National Ocean and Atmospheric Administration (NOAA) Global Drifter Program (GDP). Successive positions of the drifter were transmitted to the R/V Marion Dufresne four times a day by the NOAA GDP center. The time-irregular positions of the drifter were interpolated into a regular time step of 12 min and a low-pass filter of 48 h was then applied to filter all tidal currents and inertial oscillations. The SVP drifter provided a

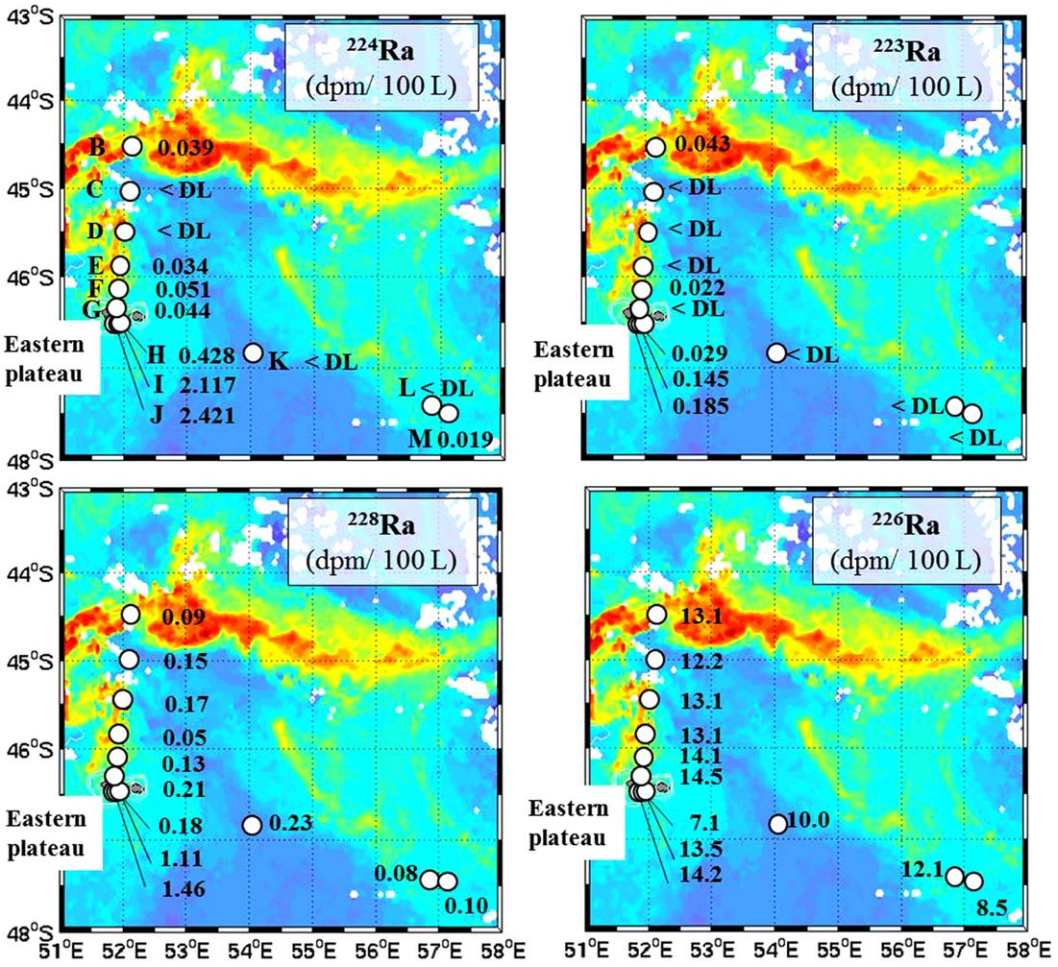

Figure 3. ^{224}Ra, ^{223}Ra, ^{228}Ra, and ^{226}Ra activities measured in surface waters off the Crozet Islands. Radium activities are reported on the chlorophyll satellite image obtained on 14 October 2011 that corresponds to the period of sampling.

measurement of mean currents in the surface mixed layer (drogue centered at 30 m depth) and information on the dispersion of water masses due to eddy activities.

2.4.4. Multisatellite Data and Lagrangian Model

During the cruise, 1/10° resolution maps of sea surface chlorophyll and 1/8° resolution maps of sea surface heights were acquired in near-real time from Ssalto/Duacs and CLS (Collecte Localisation Satellites, Toulouse, France) with support from Centre National d'Etudes Spatiales (CNES, France). These satellite products merged observations from the MODIS/MERIS and the Jason1/Jason2/ENVISAT missions, respectively. These data have been used for detecting the chlorophyll plume, siting the sampling stations, and choosing the release location for the SVP drifter. Altimetry-derived velocities providing the geostrophic, mesoscale velocity at the ocean surface were analyzed in near-real time with a Lagrangian model. These mapped altimetric velocities smooth out the smaller scale but provide a good evolution of the larger mesoscale ocean dynamics [*Dibarboure et al*., 2011]. This model was inspired by *Mongin et al*. [2009], who reconstructed the extension of the Kerguelen chlorophyll plume with a transport scheme based on altimetry. This model created thousands of virtual surface drifters whose trajectories were constructed by integrating the altimetric velocity field. The release position of "lythogenic" drifters (apparent age = 0) was set on the shelf break of Crozet (2000 m isobath). Technically, trajectories were constructed by backward-in-time integration, starting from a uniform drifter distribution spaced at 1/10° resolution. The backward-in-time integration was stopped when a hit over the Crozet shelf break was detected (indicating a trajectory coming from the shelf), or when a maximum integration time—set to 120 days—was reached (indicating no interaction with the shelf on the past 120 days).

3. Results and Discussion

3.1. Physical Characteristics of the Phytoplankton Plume

The satellite image of sea surface chlorophyll obtained on 14 October 2011 shows that the phytoplankton bloom developed north of the Crozet Islands up to 44°S (ca. 215 km distance offshore), flowed around the Crozet Plateau to the west, and finally expanded eastward (Figure 2). In Figure 2, we reported only surface currents that were averaged within the surface mixed layer (between 30 and 94 m depth) in order to compare with the radium data (samples collected at 7 m depth) and with the trajectory of the drifter (drogue centered at 30 m depth). The S-ADCP data collected along the South-North transect off Ile de la Possession show a zone of weak circulation between the Crozet Islands and 44°S, which agrees with the location of the Polar Frontal Zone (PFZ) [*Pollard et al*., 2007a]. Stronger eastward currents are observed with S-ADCP data between 42°S and 43°S, which may be associated with the SAF (Figure 1) [*Pollard et al*., 2007a]. The phytoplankton bloom was thus bounded northward and westward by the SAF.

Eleven stations were investigated across the phytoplankton plume off the Crozet Islands (Figure 2). All samples, except the northernmost sample, were collected south of the SAF in the SubAntarctic Surface Water (SASW) [*Ku and Lin*, 1976; *Orsi et al*., 1995]. According to the real-time chlorophyll satellite images, three stations were located in HNLC surface waters (i.e., below 0.5 mg m^{-3} on the chlorophyll map; stations A, C, and K). The other stations were located inside the chlorophyll plume (i.e., above 0.5 mg m^{-3} on the chlorophyll map; stations B, D, E, F, G, H, L, and M). The SST of stations located in HNLC waters was slightly lower (mean SST and SSS were 3.64 $\pm$ 0.19°C and 33.83, respectively) than the SST of stations located within the chlorophyll plume (mean SST and SSS were 4.31 $\pm$ 0.32°C and 33.86 $\pm$ 0.04, respectively). Station D displayed a SST slightly lower than that of stations located within the plume (3.93°C), suggesting that this station may be at the edge of the plume and likely under significant influence of the HNLC waters. Station A located north of the SAF displayed T-S characteristics different from all the other stations suggesting an influence of subtropical waters. Finally, the two samples collected on the beach of the Baie du Marin (stations I and J) displayed a SSS lower than that of samples collected offshore (30.560 and 31.552 for stations J and I, respectively).

The drifter that was deployed north of Ile de la Possession (Figure 2, magenta star) followed the shape of the chlorophyll plume. The drifter moved northward until the 10th day. Then, it flowed westward and reached its westernmost position on the 17th day before being swept eastward by the SAF. The drifter passed close to several stations on the northward transect (Figure 2).

3.2. Radium Activities

3.2.1. Long-Lived Radium Activities (^{228}Ra and ^{226}Ra)

The ^{226}Ra and ^{228}Ra activities reported here (Table 1) are comparable to values reported for the Southern Ocean [*Kaufman et al*., 1973; *Broecker et al*., 1976; *Ku and Lin*, 1976; *Hanfland*, 2002; *van Beek et al*., 2008]. ^{226}Ra activities in surface waters from the Southern Ocean are relatively high in comparison to surface waters of the Atlantic and Pacific Oceans [*Broecker et al*., 1967, 1976; *Chung*, 1974; *Ku and Lin*, 1976; *Chung and Craig*, 1980], because of the upwelling of deep waters that are enriched in ^{226}Ra at high latitudes [*Ku and Lin*, 1976]. Except for three low values, the ^{226}Ra activities reported here range from 10.0 to 14.5 dpm/100 L (Table 1 and Figure 3). In contrast, ^{228}Ra activities are especially low in the Southern Ocean [*Kaufman et al*., 1973]. Thus, the ^{228}Ra activities are often below the detection limit in open-ocean waters and only become significant near islands or the Antarctic continent [*Hanfland*, 2002; *Charette et al*., 2007; *van Beek et al*., 2008; *Dulaiova et al*., 2009; *Annett et al*., 2013]. The ^{228}Ra activities reported here are higher in the two samples collected at the beach of the Baie du Marin (Ile de la Possession) (Table 1 and Figure 3). The ^{228}Ra activities then decrease with increasing distance between the coast and 62 km offshore. Note, however, that the samples collected in HNLC waters outside of the chlorophyll plume sometimes exhibit relatively high values (e.g., station K).

3.2.2. Short-Lived Radium Activities (^{224}Ra and ^{223}Ra)

The ^{223}Ra and ^{224}Ra activities reported here (Table 1) are comparable to the scarce data reported in the literature for waters collected near islands located in the Southern Ocean [*Charette et al*., 2007; *Dulaiova et al*., 2009; *Annett et al*., 2013]. The highest short-lived radium activities are observed in samples I and J because they were collected in the shallow waters of the Baie du Marin. In addition, a river that discharges into the Baie du Marin as indicated by the salinity data may also contribute to the high radium activities. ^{223}Ra and ^{224}Ra activities then decrease with increasing distance from the source term (the Crozet Islands) due to radioactive decay and mixing. In the

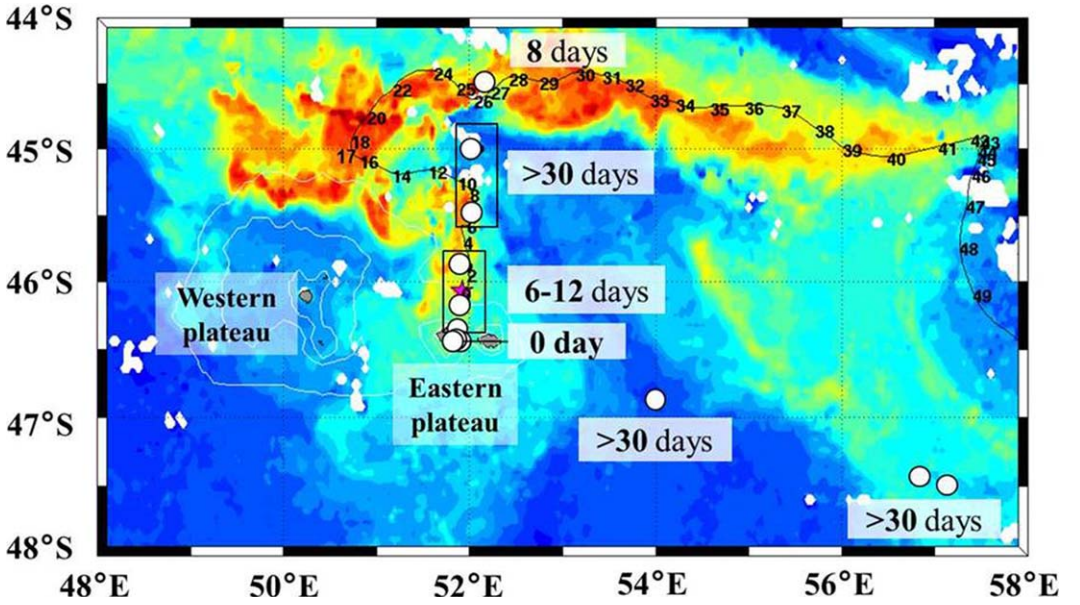

Figure 4. Apparent radium ages of surface waters derived from the $^{224}Ra/^{228}Ra$ ratios. The equivalent transit time of the drifter is reported in days along its trajectory. The magenta star shows the deployment location of the drifter.

middle of the Baie du Marin (station H), both the ^{224}Ra and ^{223}Ra activities have already decreased by a factor of 5. The $^{224}Ra/^{228}Ra$ and $^{224}Ra/^{223}Ra$ ratios, however, are in a narrow range at the three stations investigated in the bay (stations H, I, and J; Table 1). This suggests that mixing and not radioactive decay is the factor controlling the decrease in the activities within the Baie du Marin. Then the ^{224}Ra activity has decreased an another factor of 10 at station G that is located 12 km offshore. The ^{224}Ra activities remain relatively uniform between 12 km (station G) and 62 km (station E) offshore while on that latter section, a significant ^{223}Ra activity could be detected only at station F. North of 62 km offshore, both ^{223}Ra and ^{224}Ra activities are below the detection limit. However, although it was located around 200 km from Ile de la Possession, station B displays significant ^{223}Ra and ^{224}Ra activities. These higher activities are located within the chlorophyll plume that expanded eastward, and suggest the trace of waters that recently interacted with shelf sediments. The ^{223}Ra and ^{224}Ra activities observed at station B, however, are not accompanied by a significantly higher ^{228}Ra activity. Regarding the south-east transect, stations K, L, and M exhibit ^{223}Ra and ^{224}Ra activities below/or close to the detection limit (Figure 3).

3.3. Offshore Transport Between the Crozet Islands and the Open Ocean

3.3.1. Apparent Ages Derived From Radium Isotopes

The radium distribution along the coast-offshore transect can provide information on the time scales of the transport between the coast and offshore waters. First, the presence of ^{224}Ra and ^{223}Ra in offshore waters indicates that the waters have recently been in interaction with the sediments (<1 month for ^{224}Ra and <3 months for ^{223}Ra). More quantitatively, radium isotopes can be used to determine the apparent ages of surface waters. Apparent ages can be calculated from the $^{224}Ra/^{228}Ra$ ratios determined in each water sample as follows [*Moore*, 2000b; *Dulaiova and Burnett*, 2008; *Dulaiova et al.*, 2009]

$$t = \ln\left[\left(^{224}Ra/^{228}Ra\right)_i / \left(^{224}Ra/^{228}Ra\right)_{obs}\right]\left(\lambda_{224} - \lambda_{228}\right)^{-1} \quad (1)$$

where $(^{224}Ra/^{228}Ra)_i$ is the initial ratio, $(^{224}Ra/^{228}Ra)_{obs}$ is the ratio for a given water sample, and λ_{224} and λ_{228} are the decay constants of ^{224}Ra and ^{228}Ra, respectively. The $^{224}Ra/^{228}Ra$ (and $^{224}Ra/^{223}Ra$) ratios determined in samples collected in the Baie du Marin at stations I and J (beach) and H (middle of the bay) are in a close range (Table 1). For this reason, we used the mean of these ratios as the initial $^{224}Ra/^{228}Ra$ ratio. We assumed that all the surface water samples had the same initial ratio and that the distribution of radium activities was only affected by radioactive decay and mixing (Figure 4). When ^{223}Ra activities could be detected, apparent ages were also determined from the $^{224}Ra/^{223}Ra$ ratios using the same assumptions as described above (Table 1). Because of the relatively large uncertainties associated with several ^{223}Ra and

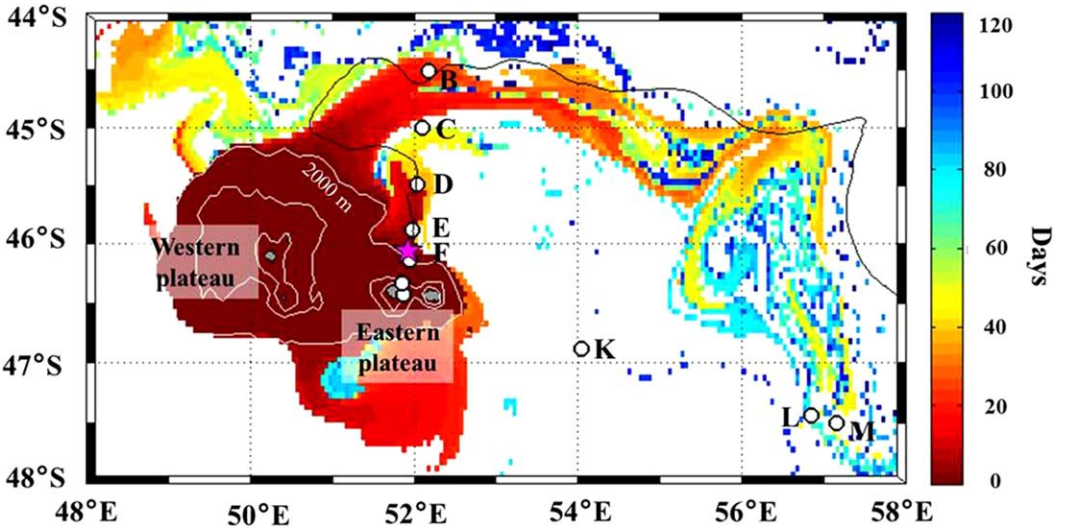

Figure 5. Ages of surface waters derived from the model based on altimetry data. Solid white lines mark the 200, 500, and 2000 m bathymetric contours. The initial age (age = 0) is considered for surface waters lying above the 2000 m isobath. White dots show the station locations.

^{224}Ra activities in open-ocean waters, the uncertainties associated with the apparent ages are also large (Table 1).

The ^{224}Ra activities that are below the detection limit at stations C, D, K, and L imply that surface waters at these stations have not been recently in contact with the sediments. For these samples, we reported "$>$ 30 days" in order to indicate that the geochemical signature of the water is old (Figure 4). In contrast, water samples displaying significant ^{224}Ra indicate a relatively recent interaction with shallow sediments or a recent input of ^{224}Ra. Apparent ages of samples collected between 12 and 62 km distance from Ile de la Possession (stations G, F, and E) are in a close range (6 $\pm$ 5 to 12 $\pm$ 4 days; Figure 4). The apparent age derived from the ^{224}Ra/^{223}Ra ratio at station F located 34 km off Ile de la Possession (14 $\pm$ 6 days) agrees with the age deduced from the ^{224}Ra/^{228}Ra ratio (9 $\pm$ 4 days). In contrast, although stations G and E displayed significant ^{224}Ra activities, no significant ^{223}Ra activities were determined in these samples (Table 1). The geochemical signature of waters collected at stations C and D is old considering that no significant ^{224}Ra and ^{223}Ra activities were determined in these samples. Finally, the apparent age determined using the ^{224}Ra/^{228}Ra ratio at station B, within the phytoplankton plume at ca. 214 km distance from Ile de la Possession, is 8 $\pm$ 8 days. The apparent age determined at station B using the ^{224}Ra/^{223}Ra ratio is slightly higher (21 $\pm$ 12 days) but both ages suggest a recent interaction with the shelf sediments.

3.3.2. Comparison of the Apparent Radium Ages With In Situ Data Derived From the Drifter

The apparent radium ages can be compared with the ages derived from the drifter that was deployed north of Ile de la Possession and that passed close to several stations investigated in this study (Figure 4). The drifter reached a distance of 62 km offshore (station E) 3 days after its deployment, which is on the same order of magnitude with the radium apparent age (6 $\pm$ 5 days). The drifter then reached the latitude of station D 7 days after it was released. The radium apparent age at station D is "$>$30 days." However, the T-S characteristics at station D suggested that this stations might be under significant influence of the HNLC waters that flow northward, which could explain why no significant ^{223}Ra and ^{224}Ra activities were detected at this station. Note also that the drifter was deployed north of our zero-age end-member used to estimate the apparent Ra ages (Figure 4), which results in an offset of a few days between the two estimates. For this reason, we also estimated the mean velocity along the northern section in order to better compare the two data sets. The mean northward velocity (and associated standard deviation) deduced from the drifter data for the first 10 days of the drift is 11.5 $\pm$ 6.1 cm s^{-1}. This value agrees with the velocity of 5–11 cm s^{-1} derived from the radium ages between the island and 62 km offshore.

The drifter reached station B 27 days after it was released (Figure 4), which agrees with the apparent radium age determined at this station using the $^{224}Ra/^{223}Ra$ ratio (21 ± 12 days). The apparent radium age determined using the $^{224}Ra/^{228}Ra$ ratio at this station is younger (8 ± 8 days). This latter apparent age is younger than (i) the drifter data and (ii) the stations located along the transect further south (D, E, and F). The transit time given by the drifter (27 days) suggests that the ^{224}Ra activity determined at station B could not originate from the eastern plateau, since the drifter transit time is more than seven times the ^{224}Ra half-life. The discrepancy between the two ages (drifter versus Ra isotopes) suggests that station B likely received a recent input of radium, which could not have come from the eastern plateau along the drifter pathway. The shallow sediments located north of the western Crozet Plateau (ca. 51°E; 45.5°S) likely supplied radium to the surface waters found at station B, thus yielding the young apparent age. If we assume that the initial $^{224}Ra/^{228}Ra$ ratio on the western plateau is similar to that of the eastern plateau, then this implies that the transit time of the waters between the western plateau and station B was around 8 days, which is in good agreement with the transit time given by the drifter between these two locations ($\Delta t = 27 - 17 = 10$ days; Figure 4). This pattern suggests that the shallow sediments of the western Crozet Plateau should be considered as a source of radium, iron, and other micronutrients, as well as the sediments from the eastern plateau. Because of the large error bar associated with the apparent age determined using the $^{224}Ra/^{223}Ra$ ratio, the value of (21 ± 12 days) does not contradict this scenario.

Twenty-five days later, the drifter reached 58°E–46.5°S (400 km southeast of the eastern plateau), close to stations L and M. These latter stations were investigated because they were located in the chlorophyll plume that expands eastward (Figure 4). However, ^{223}Ra and ^{224}Ra activities were not significant at these stations.

3.3.3. Apparent Ages Derived From an Altimetry-Based Lagrangian Model

The time scales taken by coastal surface waters to be advected offshore were also investigated using an altimetry-based Lagrangian model (Figure 5). The color bar indicates the time (number of days) elapsed since the water body left the 2000 m isobath. Note that the large standard deviations associated with the ages estimated with this Lagrangian advection model reflect the strong variability of the surface water ages in that area (Table 1). The distribution of the virtual drifters originating from the shelves of the Crozet Island is remarkably similar to the shape of the chlorophyll plume (Figures 2 and 5). There is also a good agreement between the model outputs and the drifter path (Figure 5). This observation highlights the key role played by surface horizontal transport in defining the extension of the spring-time chlorophyll plume. This pattern agrees with the conclusion of previous studies conducted in the region of the Crozet Islands [*Pollard et al*., 2007a] and in the Kerguelen region [*Mongin et al*., 2009].

Stations F, G, H, I, and J were located in the area delimited by the 2000 m isobath contour (i.e., within the area defined as the zero-age end-member). The white color in Figure 5 indicates areas that are located outside the numerical plume, suggesting that the maximum integration time of 120 days was reached at these locations (we reported "$>$120 days" in Table 1). Stations C, K, M, and A are located within this area. This pattern agrees with the apparent radium ages that also suggested an old geochemical signature for these waters (Figure 4).

The Lagrangian advection model shows two different paths of shelf-derived waters that flowed northward: one flow originating from the eastern Crozet Plateau and the other flow originating from the western Crozet Plateau. This pattern agrees with the conclusion derived from the distribution of the ^{224}Ra activities. The model confirmed transport between the shelf and offshore on the northern transect. The model suggests that station E (62 km) is reached after 9 ± 11 days and station D after 27 ± 15 days, which agrees with the apparent radium ages determined at these stations (6 ± 5 and >30 days, respectively). For station B, located in the northernmost extension of the plume, the model provides an age of 21 ± 2 days (Figure 5 and Table 1), which is the transport time of the water body that detached from the western plateau. Young apparent ages were also determined at station B using Ra isotopes considering the western plateau as a source term (8 ± 8 and 21 ± 12 days derived from the $^{224}Ra/^{228}Ra$ and $^{224}Ra/^{223}Ra$ ratios, respectively). The drifter data are also in agreement taking around 10 days to drift between the western plateau and station B (Figure 4). We conclude that there is a reasonably good agreement between the different methods, considering (i) the errors associated with each method and (ii) that the transit times were not investigated on exactly the same distances. Finally, the apparent age derived by the model for station L, located southeast

of the Crozet Islands, is 72 ± 8 days. With such a transit time, no remaining ^{223}Ra and ^{224}Ra are expected at these stations, which is also consistent with the apparent radium ages.

4. Conclusion

The use of three independent methods—including geochemical and physical methods—allowed us to validate each method (i.e., estimate of apparent ages using radium isotopes or using a satellite-derived transport model). When combined, the different methods allowed us to assess the rates and time scales for the offshore transport of surface waters and to give information on the origin of iron fertilization in this region of the Southern Ocean. The shelf-water contact ages derived from the radium isotopes and from the different physical methods (SVP Lagrangian drifter and satellite-derived transport model) are in relatively good agreement with each other and converged to the same conclusions. We showed that the Crozet Island phytoplankton plume is fed by two different flows of water that interacted with either the western plateau or the eastern plateau. Our data suggest a relatively fast offshore transport north of Ile de la Possession on the eastern plateau (60 km is reached within 1–2 weeks, which is equivalent to a velocity of 5–11 cm s^{-1}), while the transit time between the western plateau and station B is on the order of 8–21 days. The transport rates determined in this study can be used, for example, to better constrain (i) the response of the ecosystems (e.g., phytoplankton, bacteria) to the input of the iron released by the shelves and (ii) the kinetics of chemical reactions that take place during this transportation (e.g., release of iron associated particles into the dissolved phase).

Acknowledgments

The authors would like to thank Bernard Quéguiner, chief scientist of the KEOPS-2 cruise. We thank the captain and crew members of the R/V Marion Dufresne. We are especially grateful to Pierre Sangiardi (IPEV) who designed the pump that allowed us to collect surface water samples in this project. We are grateful to Sarah Nicholas and Rosemary Morrow for constructive discussions on the manuscript. We thank EDF for kindly allowing us to place our gamma detectors in the tunnel of Ferrières (Ariège, French Pyrénées). The altimeter and color/temperature products for the Kerguelen area were produced by Ssalto/Duacs (http://www.aviso.oceanobs.com/en/data/product-information/duacs/) and CLS (http://www.cls.fr/welcome_en.html) with support from CNES. We thank Laurent Testut for providing the data of the tidal model MOG2D. This work was funded by ANR (ANR-2010-BLAN-614), IPEV, and INSU/CNRS. The altimetry-based Lagrangian analysis is a contribution to the OSTST ALTIMECO project. We thank Bradley Moran, Editor, and the two anonymous reviewers for their constructive comments that allowed us to improve significantly the quality of the paper.

References

Annett, A. L., S. F. Henley, P. Van Beek, M. Souhaut, R. Ganeshram, H. J. Venables, M. P. Meredith, and W. Geibert (2013), Use of radium isotopes to estimate mixing rates and trace sediment inputs to surface waters in northern Marguerite Bay, Antarctic Peninsula, *Antarct. Sci.*, *25*, 445–456, doi:10.1017/S0954102012000892.

Banse, K. (1996), Low seasonality of low concentrations of surface chlorophyll in the subantarctic water ring: Underwater irradiance, iron, or grazing?, *Prog. Oceanogr.*, *37*(3–4), 241–291, doi:10.1016/S0079-6611(96)00006-7.

Blain, S., et al. (2001), A biogeochemical study of the island mass effect in the context of the iron hypothesis: Kerguelen Islands, Southern Ocean, *Deep Sea Res., Part I*, *48*(1), 163–187, doi:10.1016/S0967-0637(00)00047-9.

Blain, S., et al. (2007), Effect of natural iron fertilization on carbon sequestration in the Southern Ocean, *Nature*, *446*(7139), 1070–1074, doi:10.1038/nature05700.

Boyd, P. W. (2002), The role of iron in the biogeochemistry of the Southern Ocean and equatorial Pacific: A comparison of in situ iron enrichments, *Deep Sea Res., Part II*, *49*(9–10), 1803–1821, doi:10.1016/S0967-0645(02)00013-9.

Boyd, P. W., et al. (2000), A mesoscale phytoplankton bloom in the polar Southern Ocean stimulated by iron fertilization, *Nature*, *407*(6805), 695–702, doi:10.1038/35037500.

Broecker, W. S., Y. H. Li, and J. Cromwell (1967), Radium-226 and Radon-222: Concentration in Atlantic and Pacific Oceans, *Science*, *158*(3806), 1307–1310, doi:10.1126/science.158.3806.1307.

Broecker, W. S., J. Goddard, and J. L. Sarmiento (1976), The distribution of 226Ra in the Atlantic Ocean, *Earth Planet. Sci. Lett.*, *32*(2), 220–235, doi:10.1016/0012-821X(76)90063-7.

Castrillejo, M., P. J. Statham, G. R. Fones, H. Planquette, F. Idrus, and K. Roberts (2013), Dissolved trace metals (Ni, Zn, Co, Cd, Pb, Al, and Mn) around the Crozet Islands, Southern Ocean, *J. Geophys. Res. Oceans*, *118*, 5188–5201, doi:10.1002/jgrc.20359.

Charette, M. A., K. O. Buesseler, and J. E. Andrews (2001), Utility of radium isotopes for evaluating the input and transport of ground-water-derived nitrogen to a Cape Cod estuary, *Limnol. Oceanogr.*, *46*(2), 465–470.

Charette, M. A., M. E. Gonneea, P. J. Morris, P. Statham, G. Fones, H. Planquette, I. Salter, and A. N. Garabato (2007), Radium isotopes as tracers of iron sources fueling a Southern Ocean phytoplankton bloom, *Deep Sea Res., Part II*, *54*(18–20), 1989–1998, doi:10.1016/j.dsr2.2007.06.003.

Chung, Y.-C. (1974), Radium-226 and Ra-Ba relationships in Antarctic and Pacific waters, *Earth Planet. Sci. Lett.*, *23*(1), 125–135, doi:10.1016/0012-821X(74)90039-9.

Chung, Y.-C., and H. Craig (1980), 226Ra in the Pacific Ocean, *Earth Planet. Sci. Lett.*, *49*(2), 267–292, doi:10.1016/0012-821X(80)90072-2.

Coale, K. H., et al. (1996), A massive phytoplankton bloom induced by an ecosystem-scale iron fertilization experiment in the equatorial Pacific Ocean, *Nature*, *383*(6600), 495–501, doi:10.1038/383495a0.

De Baar, H. J. W., J. T. M. de Jong, D. C. E. Bakker, B. M. Löscher, C. Veth, U. Bathmann, and V. Smetacek (1995), Importance of iron for plankton blooms and carbon dioxide drawdown in the Southern Ocean, *Nature*, *373*(6513), 412–415, doi:10.1038/373412a0.

Dibarboure, G., M.-I. Pujol, F. Briol, P. Y. L. Traon, G. Larnicol, N. Picot, F. Mertz, and M. Ablain (2011), Jason-2 in DUACS: Updated system description, first tandem results and impact on processing and products, *Mar. Geod.*, *34*(3–4), 214–241, doi:10.1080/01490419.2011.584826.

Dulaiova, H., and W. C. Burnett (2008), Evaluation of the flushing rates of Apalachicola Bay, Florida via natural geochemical tracers, *Mar. Chem.*, *109*(3–4), 395–408.

Dulaiova, H., M. V. Ardelan, P. B. Henderson, and M. A. Charette (2009), Shelf-derived iron inputs drive biological productivity in the southern Drake Passage, *Global Biogeochem. Cycles*, *23*, GB4014, doi:10.1029/2008GB003406.

Emery, W. J., and J. Meincke (1986), Global water masses: Summary and review, *Oceanol. Acta*, *9*(4), 383–391.

Frost, B. W. (1991), The role of grazing in nutrient-rich areas of the open sea, *Am. Soc. Limnol. Oceanogr.*, *36*(8), 1616–1630.

Garcia-Solsona, E., J. Garcia-Orellana, P. Masqué, and H. Dulaiova (2008), Uncertainties associated with 223Ra and 224Ra measurements in water via a Delayed Coincidence Counter (RaDeCC), *Mar. Chem.*, *109*(3–4), 198–219, doi:10.1016/j.marchem.2007.11.006.

Hanfland, C. (2002), Radium-226 and Radium-228 in the Atlantic Sector of the Southern Ocean, thesis, Alfred Wegener Inst., Bremerhaven, Germany.
Kaufman, A., R. M. Trier, W. S. Broecker, and H. W. Feely (1973), Distribution of 228Ra in the world ocean, *J. Geophys. Res.*, *78*(36), 8827–8848, doi:10.1029/JC078i036p08827.
Korb, R. E., and M. Whitehouse (2004), Contrasting primary production regimes around South Georgia, Southern Ocean: Large blooms versus high nutrient, low chlorophyll waters, *Deep Sea Res., Part I*, *51*(5), 721–738, doi:10.1016/j.dsr.2004.02.006.
Korb, R. E., M. J. Whitehouse, and P. Ward (2004), SeaWiFS in the southern ocean: Spatial and temporal variability in phytoplankton biomass around South Georgia, *Deep Sea Res., Part II*, *51*(1–3), 99–116, doi:10.1016/j.dsr2.2003.04.002.
Ku, T.-L., and M.-C. Lin (1976), 226Ra distribution in the Antarctic Ocean, *Earth Planet. Sci. Lett.*, *32*(2), 236–248, doi:10.1016/0012-821X(76)90064-9.
Lucas, M., S. Seeyave, R. Sanders, C. Mark Moore, R. Williamson, and M. Stinchcombe (2007), Nitrogen uptake responses to a naturally Fe-fertilised phytoplankton bloom during the 2004/2005 CROZEX study, *Deep Sea Res., Part II*, *54*(18–20), 2138–2173.
Maraldi, C., B. Galton-Fenzi, F. Lyard, L. Testut, and R. Coleman (2007), Barotropic tides of the Southern Indian Ocean and the Amery Ice Shelf cavity, *Geophys. Res. Lett.*, *34*, L18602, doi:10.1029/2007GL030900.
Martin, J. H., S. E. Fitzwater, and R. M. Gordon (1990), Iron deficiency limits phytoplankton growth in Antarctic waters, *Global Biogeochem. Cycles*, *4*(1), 5–12, doi:10.1029/GB004i001p00005.
Mitchell, B. G., E. A. Brody, O. Holm-Hansen, C. McClain, and J. Bishop (1991), Light limitation of phytoplankton biomass and macronutrient utilization in the Southern Ocean, *Limnol. Oceanogr.*, *36*(8), 1662–1677.
Mongin, M. M., E. R. Abraham, and T. W. Trull (2009), Winter advection of iron can explain the summer phytoplankton bloom that extends 1000 km downstream of the Kerguelen Plateau in the Southern Ocean, *J. Mar. Res.*, *67*(2), 225–237, doi:10.1357/002224009789051218.
Moore, W. S. (2000a), Ages of continental shelf waters determined from 223Ra and 224Ra, *J. Geophys. Res.*, *105*(C9), 22,117–22,122, doi:10.1029/1999JC000289.
Moore, W. S. (2000b), Determining coastal mixing rates using radium isotopes, *Cont. Shelf Res.*, *20*(15), 1993–2007, doi:10.1016/S0278-4343(00)00054-6.
Moore, W. S. (2008), Fifteen years experience in measuring 224Ra and 223Ra by delayed-coincidence counting, *Mar. Chem.*, *109*(3–4), 188–197, doi:10.1016/j.marchem.2007.06.015.
Moore, W. S., and R. Arnold (1996), Measurement of 223Ra and 224Ra in coastal waters using a delayed coincidence counter, *J. Geophys. Res. 101*(C1), 1321–1329, doi:10.1029/95JC03139.
Orsi, A. H., T. Whitworth III, and W. D. Nowlin Jr. (1995), On the meridional extent and fronts of the Antarctic Circumpolar Current, *Deep Sea Res., Part I*, *42*(5), 641–673, doi:10.1016/0967-0637(95)00021-W.
Planquette, H., et al. (2007), Dissolved iron in the vicinity of the Crozet Islands, Southern Ocean, *Deep Sea Res., Part II*, *54*(18–20), 1999–2019, doi:10.1016/j.dsr2.2007.06.019.
Pollard, R., M. Lucas, and J. Read (2002), Physical controls on biogeochemical zonation in the Southern Ocean, *Deep Sea Res., Part II*, *49*(16), 3289–3305, doi:10.1016/S0967-0645(02)00084-X.
Pollard, R., R. Sanders, M. Lucas, and P. Statham (2007a), The Crozet Natural Iron Bloom and Export Experiment (CROZEX), *Deep Sea Res., Part II*, *54*(18–20), 1905–1914, doi:10.1016/j.dsr2.2007.07.023.
Pollard, R. T., and J. F. Read (2001), Circulation pathways and transports of the Southern Ocean in the vicinity of the Southwest Indian Ridge, *J. Geophys. Res.*, *106*(C2), 2881–2898, doi:10.1029/2000JC900090.
Pollard, R. T., H. J. Venables, J. F. Read, and J. T. Allen (2007b), Large-scale circulation around the Crozet Plateau controls an annual phytoplankton bloom in the Crozet Basin, *Deep Sea Res., Part II*, *54*(18–20), 1915–1929, doi:10.1016/j.dsr2.2007.06.012.
Seeyave, S., M. I. Lucas, C. M. Moore, and A. J. Poulton (2007), Phytoplankton productivity and community structure in the vicinity of the Crozet Plateau during austral summer 2004/2005, *Deep Sea Res., Part II*, *54*(18–20), 2020–2044, doi:10.1016/j.dsr2.2007.06.010.
van Beek, P., M. Bourquin, J.-L. Reyss, M. Souhaut, M. A. Charette, and C. Jeandel (2008), Radium isotopes to investigate the water mass pathways on the Kerguelen Plateau (Southern Ocean), *Deep Sea Res., Part II*, *55*(5–7), 622–637, doi:10.1016/j.dsr2.2007.12.025.
van Beek, P., M. Souhaut, and J.-L. Reyss (2010), Measuring the radium quartet (228Ra, 226Ra, 224Ra, 223Ra) in seawater samples using gamma spectrometry, *J. Environ. Radioactiv.*, *101*(7), 521–529, doi:10.1016/j.jenvrad.2009.12.002.
van Beek, P., M. Souhaut, B. Lansard, M. Bourquin, J.-L. Reyss, P. von Ballmoos, and P. Jean (2013), LAFARA: A new underground laboratory in the French Pyrenees for ultra low-level gamma-ray spectrometry, *J. Environ. Radioactiv.*, *116*, 152–158, doi:10.1016/j.jenvrad.2012.10.002.
Venables, H. J., R. T. Pollard, and E. E. Popova (2007), Physical conditions controlling the development of a regular phytoplankton bloom north of the Crozet Plateau, Southern Ocean, *Deep Sea Res., Part II*, *54*(18–20), 1949–1965, doi:10.1016/j.dsr2.2007.06.014.